Analysing the influence of finite deformations treatment towards the safety assessment of nuclear waste repositories

Steffen Beese
Federal Institute for Geoscience and Natural Resources, Hannover, Germany

Ralf Eickemeier
Federal Institute for Geoscience and Natural Resources, Hannover, Germany

Jobst Maßmann
Federal Institute for Geoscience and Natural Resources, Hannover, Germany

Sandra Fahland
Federal Institute for Geoscience and Natural Resources, Hannover, Germany

ABSTRACT: In the analysis of underground disposals over multiple thousands of years the assumption of small strains can be violated. In this contribution an extension of the BGRc creep model to the finite deformation regime is outlined.
With small scale examples the finite deformation treatment of the underlying boundary value problem is studied towards its influence on safety assessments for geological nuclear waste repositories.

Keywords: Finite Deformation, Rock Salt, Creep, Finite Element Method.

1 INTRODUCTION

In order to find a safe and reliable geological disposal site for high-level radioactive waste, rock salt formations are important candidates as corresponding host rock. The mechanical advantages such as high ductility, its tightness and the large undisturbed volumes as well as its capacity to heal out fractures compete with its disadvantages such as water solubility. For the dimensioning, the safety assessment of the operational phase and its long term safety, the thermo-hydro-mechanical state of the disposal site and the surrounding rock must be predicted up to many thousands of years. Therefore, it is crucial to have reliable material models on the one hand and accurate and efficient numerical frameworks to solve the mathematical model on the other hand. The mechanical behaviour of salt has been investigated intensively in the last decades and different monographs and collections are dedicated to it. Without trying to give a comprehensive list the reader is referenced e.g. Cristescu & Hunsche (1998) or Hampel et. al. (2016).

With the excavation of disposal sites the stress state of the host rock is disturbed. Due to creep, this stress fluctuation decrease over the time, leading to deformations in the host rock. The excavated cavities will converge over a long time scale. By taking such long time scales into account the predicted deformations cannot be postulated as small. Therefore, in this contribution an attempt is made to outline the extension of a present creep law into a finite deformation context. Furthermore, the small-scale version and the large deformation one are compared by evaluation of a numerical laboratory-scale test and a generic deposition site.

2 CONSTITUTIVE MODEL FOR ROCK SALT: BGRC AT SMALL STRAINS

2.1 Creep deformation in rock salt

In this section only a rather rough overview over the small strain constitutive model for rock salt is given. The deformation of rock salt is mainly characterized by a visco-plastic behaviour. This phenomenon is known as creep and can be subdivided into three phases according to the different behaviour of a specimen observed in creep tests. These phases are denoted primary or transient creep, secondary or stationary creep and tertiary creep. In the following section the simple BGRc model is described. Here, only the transient and stationary creep phase without healing and damage is addressed. The model is capable to address dilatancy effects and solution-precipitation creep in a simplified manner.

The BGRc creep model is embedded in a standard visco-plastic setting with additive split of the small strain tensor $\boldsymbol{\epsilon}$:

$$\boldsymbol{\varepsilon} = \nabla_{\text{sym}}\mathbf{u} = \boldsymbol{\varepsilon}^{\text{p}} + \boldsymbol{\varepsilon}^{\text{e}} \tag{1}$$

into an elastic part $\boldsymbol{\varepsilon}^{\text{e}}$ and a plastic part $\boldsymbol{\varepsilon}^{\text{p}}$. The stress $\boldsymbol{\sigma}$ is defined as the partial derivative of a free HELMHOLTZ-energy-density function ψ with respect to the elastic strains:

$$\boldsymbol{\sigma} = \frac{\partial \psi}{\partial \boldsymbol{\varepsilon}^{\text{e}}} \,. \tag{2}$$

the plastic flow rule of the BGRc model is defined as:

$$\dot{\boldsymbol{\varepsilon}}^{\text{p}} := \dot{\gamma}_{\text{dev}} \frac{\boldsymbol{\sigma}_{\text{dev}}}{||\boldsymbol{\sigma}_{\text{dev}}||} + \dot{\gamma}_{\text{vol}}\mathbf{1} \,, \tag{3}$$

with $\dot{\gamma}_{\text{dev}}$ and $\dot{\gamma}_{\text{vol}}$ as the scalar creep rates. The deviatoric creep rate $\dot{\gamma}_{\text{dev}}$ is defined by:

$$\dot{\gamma}_{\text{dev}} := A_1 \exp\left(\frac{Q_1}{R \cdot T}\right)\left(\frac{\sigma_{\text{eqv}}}{\sigma^*}\right)^{n_1} + A_2 \exp\left(\frac{Q_2}{R \cdot T}\right)\left(\frac{\sigma_{\text{eqv}}}{\sigma^*}\right)^{n_2} \,. \tag{4}$$

Here, σ_{eqv} is the equivalent stress measure and T is the absolute temperature. All material parameters are summarized for convenience in table 1. The evolution law for the deviatoric creep rate $\dot{\gamma}_{\text{dev}}$ is decomposed in two NORTON-HOFF creep terms. The first term is used to model the stationary creep whereas the second term is used to model the pressure precipitation creep by setting $n_2 \approx 1$. The equivalent stress σ_{eqv} in equation (4) is defined as:

$$\sigma_{\text{eqv}} = \sigma_{\text{vM}} - \sigma_{\text{H}} \tag{5}$$

and reduces to the von MISES stress σ_{vM} in the absence of the hardening stress σ_{H}. If dislocations pile up, the hardening stress increases and the creep rate decreases. Transient creep can be interpreted as the competing mechanism of dislocation storage and recovery. In Kocks (1976) an evolution equation of the dislocation density is derived. Based on this a micromechanical motivated isotropic hardening model is used within the BGRc model. The evolution equation for the hardening stress σ_{H} then reads:

$$\dot{\sigma_{\text{H}}} = \kappa_{\text{H}}\left(\frac{\sigma_{\text{eqv}}}{\sigma_{\text{H}}} - \frac{(1-z)^2}{z^2}\frac{\sigma_{\text{H}}}{\sigma_{\text{eqv}}}\right)\dot{\gamma}_{\text{dev}} \,. \tag{6}$$

In order to obtain the same stationary creep rate as for the non-hardening case, the normalizing stress σ^* in (4) is defined to be:

$$\sigma^* = (1 - z)\sigma_0 \ . \tag{7}$$

Here, σ_0 ensures a unit independent formulation of the creep rate. The volumetric part $\dot{\gamma}_{\mathrm{vol}}$ of the creep rate reflects the volume increase due to micro cracking. The dilatant behaviour is only active if the stress state is above the dilatancy boundary σ_{dil} according to Hunsche & Hampel (1999). The evolution of the volumetric creep is defined to be proportional to the deviatoric creep rate:

$$\dot{\gamma}_{\mathrm{vol}} = \frac{r_{\mathrm{v}}}{3}\dot{\gamma}_{\mathrm{dev}} \quad \text{with} \quad r_{\mathrm{v}} := \begin{cases} \min\left[a\left(\dfrac{\sigma_{\mathrm{eqv}} - \sigma_{\mathrm{dil}}}{S}\right)^{m}, r_{\mathrm{v}}^{\max}\right] & : \sigma_{\mathrm{vM}} > \sigma_{\mathrm{dil}} \\ 0 & : \sigma_{\mathrm{vM}} \leq \sigma_{\mathrm{dil}} \end{cases} . \tag{8}$$

The proportionality factor r_{v} increases with the distance to the dilatancy boundary σ_{dil} up to its maximal value of $r_{\mathrm{v}}^{\max}$. For thermodynamic consistency this factor is limited by the current stress state:

$$r_{\mathrm{v}}^{\max} := -\frac{3||\sigma_{\mathrm{dev}}||}{\mathrm{tr}\,(\sigma)} \ . \tag{9}$$

The dilatancy boundary $\sigma_{\mathrm{dil}} := \hat{\sigma}_{\mathrm{dil}}(\boldsymbol{\sigma})$ is a function of the stress state. In the present model this dependency reads:

$$\hat{\sigma}_{\mathrm{dil}}(\boldsymbol{\sigma}) = \mathrm{b}S^{\mathrm{c}} \quad \text{with } S := \max\left(-\frac{\mathrm{tr}\,[\boldsymbol{\sigma}]}{3}, \sigma_{\mathrm{lim}}\right) . \tag{10}$$

Table 1. Material parameters and units of BGRc model.

Material parameter	Value	Unit	Material parameter	Value	Unit
Young`s Modulus E	25000	MPa	Poisson`s ratio	0.27	-
Activation energy Q_1	54	kJ/mol	Activation energy Q_2	54	kJ/mol
Parameter A_1	0.357	1/d	Parameter A_2	1.2	1/d
Normalizing stress σ_1^*	1	MPa	Normalizing stress σ_2^*	1	MPa
Stress exponent n_1	5	-	Stress exponent n_2	1.25	-
Gas constant R	0.0083	kJ/(mol K)	Max. dilatant stress σ_{lim}	-0.1	MPa
a	0.816	-	m	2	-
b	1.5	-	c	1.0	-
Hardening limit z	0	-	Hardening modulus κ_H	0	-

2.2 Finite deformation framework for BGRc creep

In most finite element analysis software the small strain elasto-plasticity models are implemented in an efficient way. Therefore, Cuitino & Ortiz (1992), Simo & Meschke (1993) and later Miehe et al. (2002) developed a numerical framework to reuse the small strain algorithm and preserving the quadratic convergence of the non-linear equation solver.

The key lies in the usage of the logarithmic strain space. With this a formally identical structure of the kinematical quantities is obtained which allows the usage of the small strain constitutive models with only minor modifications. The necessary steps for the stress update were summarized by Miehe et al. (2002):

1. *Geometric pre-processing:* The logarithmic strains $\{\mathbf{E}, \mathbf{E}^{\mathrm{e}}\}$ are computed from the right CAUCHY-GREEN tensor $\mathbf{C}$ and the plastic logarithmic strains $\mathbf{E}^{\mathrm{p}}$.
2. *Stress update:* The small strain stress update algorithm is applied by interchanging the input arguments $\{\boldsymbol{\varepsilon}, \boldsymbol{\varepsilon}_{\mathrm{n}}, \boldsymbol{\varepsilon}_{\mathrm{n}}^{\mathrm{p}}\} \rightarrow \{\mathbf{E}, \mathbf{E}^{\mathrm{e}}, \mathbf{E}^{\mathrm{p}}\}$.

3. *Geometric post-processing:* Transform the resulting stress and material tangent operator to the finite deformation regime.

The implementation task for the additive plasticity model described in this section is therefore restricted to the implementation of robust and fast matrix logarithm and matrix exponential functions with the corresponding derivatives needed to compute the transformation of the stress and material tangent tensor. The presented theory was implemented into the in house FEM analysis program JIFE.

3 NUMERICAL EXAMPLES

In this section 2 numerical examples are presented. First, a multi stage triaxial test is elaborated and the differences of the small strain formulation and the large strain formulation are highlighted. The second test mimics the convergence of underground cavities. Finally the fluid pressure criterion and the dilatancy criterion are evaluated in this generic deposition site.

3.1 Deformation rate controlled laboratory test

The triaxial specimen shown in figure 1 on the left hand side is compressed with a constant strain rate $\dot{\epsilon} = 10^{-5}\ \mathrm{s}^{-1}$ and a lateral pressure $\sigma_3 = 2$ MPa. At an engineering strain of 20% the specimen is not further compressed and a stress relaxation phase takes place. The material parameters are summarized in table 1. The numerical test is carried out without hardening. In figure 1 on the right hand side the resulting stresses are plotted against the engineering strains for small deformations (SD) and for finite deformations (FDA). While the stress in the small deformation regime is constant over the entire loading phase, the finite deformation stress measure (first PIOLA-KIRCHOFF Stress) increases due to the enlargement of the corresponding area. For comparing purposes a third curve was added to figure 1. This curve was taken from figure 6 in Schulze et al. (2017). Commonly the behaviour of increasing stress in such kind of experiments are identified as hardening. But here, we can clearly see, that a significant amount of the increasing stress is related to the finite deformation treatment. For the relaxation branch of the test, the both formulations show nearly the same results.

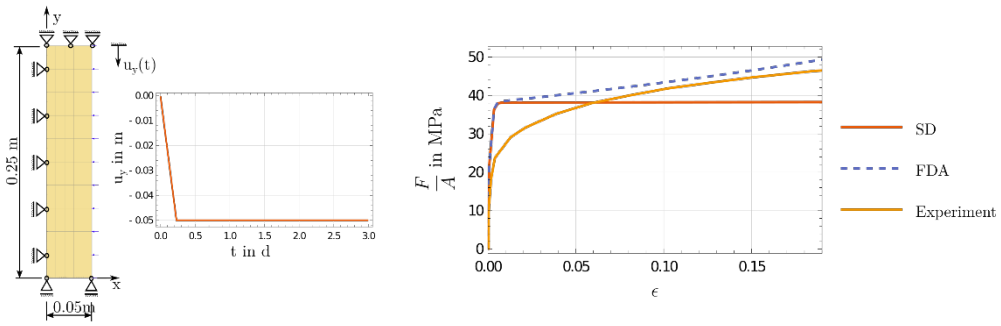

Figure 1. Boundary value problem for strain rate controlled test (left). Axial stress over strain (right).

3.2 Generic high-level radioactive waste repository

In this example a generic disposal site is modelled in two dimensions to analyse the effect of the finite deformation framework within a regime characterized by highly inhomogeneous stress states. In figure 2 the domain and its geometry are depicted. There are 4 excavations shown in the figure. Excavation E_1 is a gallery with a typical cross section area of about 21 m^2, while excavation E_2 and E_4 are disposal sites. E_2 is still fully open and E_4 is partially backfilled with an elastic material. Excavation E_3 has an unconventional geometry where the height of the gallery is larger than its width. The entire site is bedded in 4 layers of salt rock with the material parameters listed in table 2. The initial boundary value problem has symmetry boundary conditions on the left and the right hand side and the weight of the 400 m mighty and homogeneous overburden is distributed as load $\widetilde{\mathbf{T}}$. The

deformation process is simulated for 10000 years and the results of the different formulations are compared.

Table 1. Material parameters for generic geological disposal example.

	Name	E in MPa	ν	A_1 in a^{-1}	A_2 in a^{-1}	n_1	n_2
S_1	Salt 1	25e4	0.27	4.1	454	5	1.25
S_2	Salt 2	25e4	0.27	65.7	7267	5	1.25
S_3	Salt 3	25e4	0.27	16.4	1817	5	1.25
S_4	Salt 4	25e4	0.27	4.1	454	5	1.25
E_1	Excavation 1	0.1	0	-	-	-	-
E_2	Excavation 2	0.1	0	-	-	-	-
E_3	Excavation 3	0.1	0	-	-	-	-
E_4	Excavation 4	0.1	0	-	-	-	-
B_1	Backfill	15e4	0.27	-	-	-	-

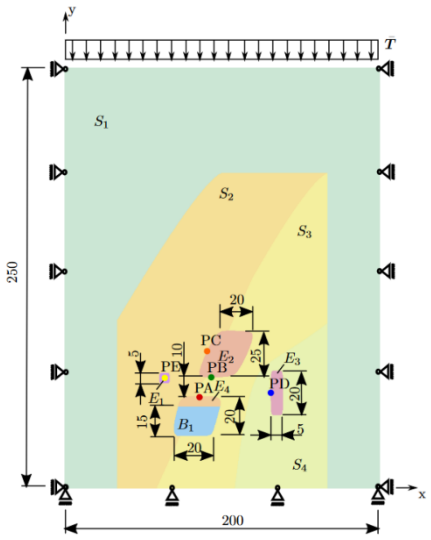

Figure 2. Boundary value problem for generic geological disposal in salt rock.

For solution times ≤ 500 years the small strain setting and the finite deformation frameworks yield nearly the same displacement. In figure 3 on the left hand side the vertical displacement of point PB is plotted over the simulation time. Here, the large strain formulation (FDA) shows a significant less downshift compared to small strain formulation (SD).

The behaviour of minor deformation can be observed in the entire model, e.g. the horizontal displacement of Point PC and PD or the convergence of excavation E_1. In figure 3 on the right hand side the von MISES stress is drawn over the line between point PA and PB at time $t = 5000$ a. Although the stress in the finite deformation simulation is generally lower, its value is higher in the vicinity of the excavation surfaces.

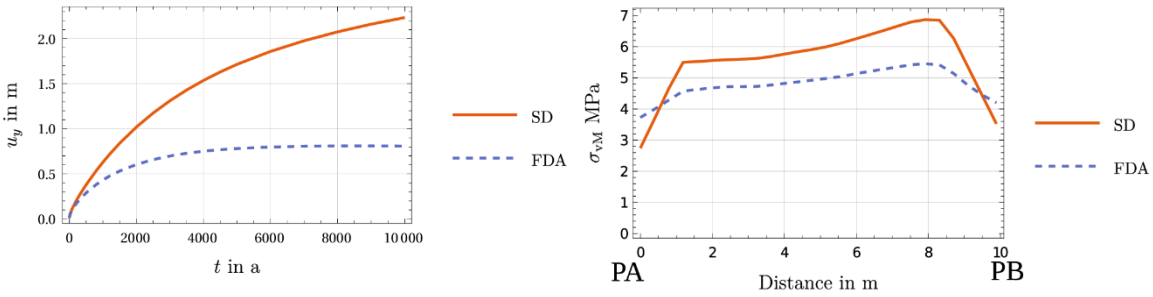

Figure 3. Vertical displacement of point PB over time (left).
Von Mises stress along line PA-PB at t = 5000 a (right).

In safety assessments a commonly used criterion for the integrity of the geological barrier is the fluid pressure criterion (Fahland et al., 2015). It states that the mean stress in the salt should be lower than the hydro-static pressure of a hypothetical water column. In figure 4 on the left hand side the zones where the criterion is not fulfilled are marked with yellow for the small strain simulation and with red for the finite deformation simulation. In the present framework these zones are nearly indistinguishable. The same holds true for the second commonly used criterion: the dilatancy criterion. In figure 4 on the right hand side the deformed configuration of the generic deposition site is shown at time $t = 5000$ a. At this time the deviatoric creep rates are already small in the finite deformation framework, which yields a slow convergence of the excavations. The red contour lines show the deformation state of the small strain simulation. Here, the convergence proceeds faster and self penetration of the finite elements must be actively prevented.

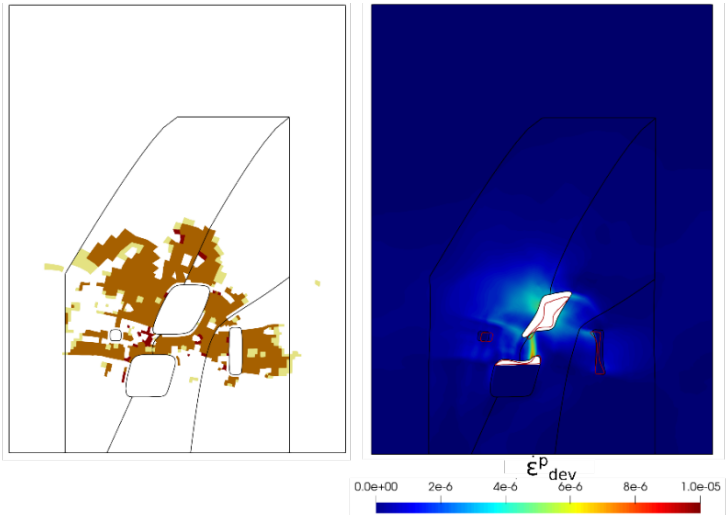

Figure 4. Zones where fluid pressure criterion is not fulfilled at t = 5000 a (left). Deviatoric creep rate for finite deformation formulation at t = 5000 a (right).

4 SUMMARY

In this contribution the constitutive setup for the current BGRc model based on the small deformation framework was outlined and a straight forward extension to the finite deformation framework was sketched. It was shown that even in laboratory experiments the usage of the finite deformation framework leads to more insight into the material behaviour. In the exemplary study of a generic repository it was shown that the solution between the two frameworks are comparable for the first 500 years. Later, the deformations are overestimated by the small strain setup. This is especially important if the sealing properties of an underground construction are studied. For the fluid pressure criterion and the dilatancy criterion no significant discrepancy could be identified in this example.

REFERENCES

Cristescu, N., & Hunsche, U. (1998). *Time effects in rock mechanics* (Vol. 350). Wiley New York.

Cuitino, A., & Ortiz, M. (1992). A material-independent method for extending stress update algorithms from small-strain plasticity to finite plasticity with multiplicative kinematics. *Engineering Computations*.

Fahland, S., Heusermann, S., & Schäfers, A. (2015). Geomechanical analysis and assessment of the integrity of the southern part in the morsleben repository. *The Mechanical Behavior of Salt VIII. Eds. Roberts, L., Mellegard, K., Hansen, F., London: Taylor & Francis*, 373–380.

Hampel, A., Herchen, K., Lux, K.-H., Günther, R.-M., Salzer, K., & Minkley, W. (2016). Comparison of advanced constitutive models and modeling procedures with model calculations of the thermo-mechanical behavior and healing of rock salt – synthesis report. *Dr. Andreas Hampel.*

Hunsche, U., & Hampel, A. (1999). Rock salt—the mechanical properties of the host rock material for a radioactive waste repository. *Engineering Geology*, *52*(3-4), 271–291.

Kocks, U. (1976). Laws for work-hardening and low-temperature creep. *J. Eng. Mater. Tech.*, *98*, 76-85.

Miehe, C., Apel, N., & Lambrecht, M. (2002). Anisotropic additive plasticity in the logarithmic strain space: Modular kinematic formulation and implementation based on incremental minimization principles for standard materials. *Computer Methods in Applied Mechanics and Engineering*, *191*(47-48), 5383–5425.

Schulze, O., Heemann, U., Zetsche, F., Hampel, A., Pudewills, A., Günther, R.-M., & others (2017). Comparison of advanced constitutive models for the mechanical behavior of rock salt–results from a joint research project–i. Modeling of deformation processes and benchmark calculations. In *The mechanical behavior of salt–understanding of thmc processes in salt* (pp. 77–88). CRC Press.

Simo, J., & Meschke, G. (1993). A new class of algorithms for classical plasticity extended to finite strains. Application to geomaterials. *Computational Mechanics*, *11*(4), 253–278.